JOURNAL OF PROPULSION AND POWER
Vol. 17, No. 3, May–June 2001

Effects of Fuel Preinjection on Mixing in Mach 1.6 Airflow

Michael Owens,* Sudarshan Mullagiri,* and Corin Segal†
University of Florida, Gainesville, Florida 32611
and
Viacheslav A. Vinogradov‡
Central Institute of Aviation Motors, 111250, Moscow, Russia

The effects of injection behind a pylon upstream of a supersonic combustion chamber were evaluated for liquid JP-10 and gaseous ethylene. A generic, rearward-facing, rectangular step was used as the primary flameholding mechanism. A pilot-hydrogen flame injected from the base of the step provided ignition. The fuel was injected from a 1.5-mm-diam wall orifice behind a thin triangular cross section pylon placed in the isolator at 10 step heights upstream of the step. The role of the pylon is to facilitate the penetration and the spreading of the liquid jet. Tests were performed under connected-pipe conditions in a Mach 1.6 airflow channel and air stagnation temperatures to 900 K, corresponding to the beginning of the hypersonic flight regime. The hydrogen, ethylene, and JP-10 flow rates were modulated during the tests and wall pressures and temperatures were measured along the duct and in the recirculation region. Shadowgraph imaging indicated the effect of injection on the isolator shock train and the combustion chamber mixing. Combustion without upstream flashback has been observed with isolator JP-10 equivalence ratios to 0.5.

Nomenclature

D	=	diameter, cm
H	=	height of rearward-facing step, 12 mm
h	=	jet penetration height, cm
P	=	pressure, KPa, MPa
q	=	dynamic pressure ratio
T	=	temperature, K
X	=	axial location, cm
Y	=	transverse location parallel to contoured sides of nozzle, cm
Z	=	transverse location perpendicular to contoured sides of nozzle, cm
η	=	efficiency
Φ	=	equivalence ratio

Subscripts

air	=	air property
C2H4	=	ethylene property
fuel	=	fuel property
H2	=	hydrogen property
inj	=	injector property
JP-10	=	JP-10 property
jet/air	=	ratio of jet/air property
mix	=	mixing
0	=	stagnation property
32	=	sauter mean diameter
∞	=	freestream property

Introduction

MIXING, vaporization of liquids, and mechanical breakup of condensed phases are all prerequisite processes for combustion. If these processes can be accomplished within the inlet, then the required residence time in the combustor can be substantially reduced, resulting in shorter combustion chambers. Furthermore, if the inlet is placed on the vehicle airframe or on the wing without using boundary-layer diverters, fuel injection can be initiated upstream of the inlet capture. The main requirements in this case are to provide fuel injection without fuel mass losses and to minimize losses of airflow impulse associated with this method of injection. Additionally, the fuel-injection scheme is to exclude the need for large supply pressures.

The danger of flashback, defined as upstream propagation of flames through boundary layers, can be eliminated in supersonic inlets if potential flameholding upstream of the combustor is avoided. This requires complete penetration of the fuel in the high-velocity airstream to avoid seeding of the boundary layer with a combustible mixture. If these conditions are satisfied, the short residence time in the inlet will preclude ignition upstream of the combustion chamber. An evaluation of the ignition delay time of a typical fuel mixture was given by Ref. 1 for stoichometric air/*n*-octane mixture as shown in Fig. 1. This analysis indicated that, for flow conditions characterized by pressures of $P_{\text{air}} = 0.05$ MPa and fuel and air temperatures of $T_{\text{fuel}} = 900$ K and $T_{\text{air}} = 900$–1100 K, respectively, the ignition time delay is $\mathcal{O}(30)$ ms. At the same time, for a typical inlet length of 1–2 m, the residence time is over two orders of magnitude less.

In general, in supersonic flow, pressure rises and flame propagates through the boundary layers, especially if fuel is present within the boundary layers. Therefore, in the case of fuel preinjection, the penetration of the fuel in the inlet boundary layer must be eliminated or reduced to concentrations below self-ignition and flameholding at the given boundary-layer temperature. This translates into the requirement of achieving sufficient fuel penetration into the airflow core. Most types of injection suggested so far include combinations of transverse and parallel injection schemes from the channel walls or by use of pylons.[2–5] Normal injection does not satisfy the need to maintain the fuel outside of the boundary layer because some fuel remains along the wall, and large relative dynamic pressure ratios $q_{\text{jet/air}}$ of the order of 10–15 are required to provide sufficient penetration depth. Injection behind pylons has the capability to increase penetration at low dynamic pressure ratios and is, thus, a more suitable option provided that the pylon aerodynamic drag is minimized.

Pylons with internal fuel channels result in a large cross section with complex internal geometry. Parallel injection from these pylons is not as efficient because the mixing lengths are 2–3

Received 5 January 2000; revision received 1 October 2000; accepted for publication 18 December 2000.

*Graduate Research Assistant, Department of Aerospace Engineering, Mechanics and Engineering Science. Student Member AIAA.
†Associate Professor, Department of Aerospace Engineering, Mechanics and Engineering Science. Member AIAA.
‡Head of Gasdynamics Department. Member AIAA.

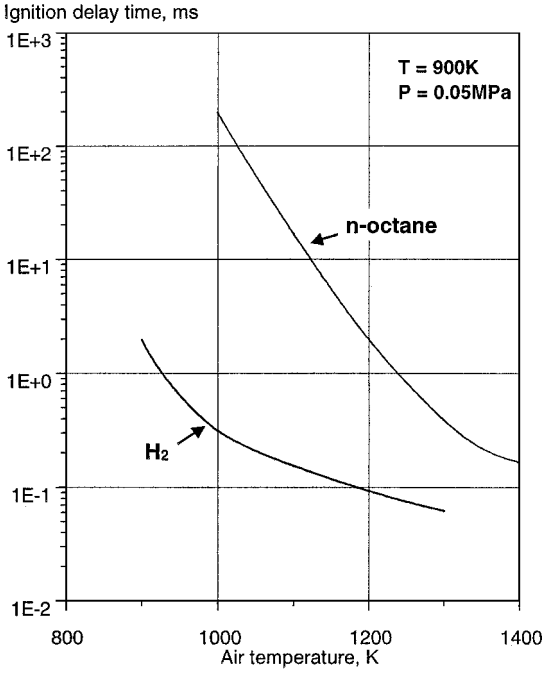

Fig. 1 Characteristic ignition delay time for H_2 and *n*-octane.[1]

times larger than for normal injection. An alternative type of injection is normal fuel injection of liquids or gases behind the pylon through a wall orifice, as described in Refs. 6 and 7. To decrease the pylon's drag, the thickness was selected as 1.5–2 times the orifice diameter D_{inj}, with swept leading edge and triangular cross section. Good penetration has been obtained with penetration heights $h/H_{pylon} = 1.3$–1.5 achieved at low dynamic pressure ratios, of the level of $q_{jet/air} = 0.5$–1.5, for both liquid[6,7] and gaseous[1] fuels. Also, good droplet atomization, $D_{32} = 4$–5 μm, of kerosene was obtained with fuel injection in Mach 2–4 flows. In the case of gaseous-fuel injection, numerical results[1] indicated high mixing efficiency with $\eta_{mix} = 0.96$–0.92 when the fuel was injected in a three-dimensional inlet at a fuel/air equivalence ratio of $\Phi = 0.2$–0.6.

In the case of fuel injection in the inlet or farther upstream, a more complex and, at the same time, a more flexible system is obtained, in which the air/fuel interactions occur over the inlet-insulator channel-combustor system. Despite the increased complexity the optimization of this system could result in significant advantages such as 1) mixing enhancement; 2) shorter isolator and combustor and, consequently, reduced weight and cooling loads; and 3) a more flexible fuel control system because there is the possibility to distribute the fuel between the preinjection system and the fuel supplied directly to the combustor, as well as the possibility to inject liquid and gaseous fuels through different sets of injectors.

The results presented hereafter constitute the continuation of the work presented in Ref. 7 on pre-injection of liquid fuel in the inlet and in the subsonic part of a Mach 1.8 nozzle.[8] It has been shown[7] that liquid injection behind two thin swept pylons at a rate corresponding to a fuel/air equivalence ratio of $\Phi = 0.2$–0.25 did not cause inlet choking, and most of the liquid penetrated into the core of the compressible flow. During connected-duct tests[8] kerosene has been injected at 10 deg relative to the wall and resulted in a rich mixture near the wall that arrived in the recirculation region of a rearward-facing step in the combustion chamber resulting in rich flameout. Therefore, in the present work, liquid JP-10 and ethylene have been injected behind a thin pylon from the isolator wall to increase penetration and improve the fuel distribution in the airflow core at air stagnation temperatures, $T_{0,air} = 300$–900 K. Combustion without flashback or upstream interaction has been achieved with isolator fuel injection up to equivalence ratios of 0.5 when flow choking was noticed due to mass addition.

Experimental Facility

The facility at University of Florida provides direct connect tests with a variable combustion chamber entrance Mach of 1.6–3.6 and stagnation temperatures corresponding to Mach 3.0–4.8 flight. All of the experiments presented here were performed with the combustion chamber entrance Mach = 1.6 and air stagnation temperatures ranging from 300 to 900 K.

The facility, shown in Fig. 2, has been described in detail elsewhere.[9] Briefly, this continuously operating facility contains a vitiated heater based on hydrogen combustion with oxygen replenishment, electronically controlled by a hybrid fuzzy logic controller to maintain a constant 0.21 oxygen mole fraction at all conditions and to maintain the constant stagnation temperature at the heater exit required for the experiment. A bellmouth with four-sided contraction leads to the supersonic nozzle with compression on two sides (i.e., two sides of the nozzle are flat and parallel to the flow axis and two sides have a contoured shape) and interchangeable nozzle blocks that cover the range of Mach 1.6–3.6. A ceramic insulation layer added on the bellmouth entrance of the nozzle produces a larger vorticity layer in the test section on the walls without compression. Figure 3 shows plots of the nozzle total pressures acquired by traversing a pitot probe across the nozzle exit, at three lateral locations, normalized by the total pressure measured in the stagnation chamber. The facility's stagnation pressure has been maintained during these tests at 4.8 atm. Although some asymmetry exits in the corners, the overall total pressure uniformity is reasonable. The total pressures indicated in Fig. 3 were recorded with an accuracy of $\pm 0.3\%$, and the static pressure measured along the test section walls were recorded with an accuracy of $\pm 0.9\%$.

A 15-cm-long constant area isolator is placed between the nozzle and the combustor section to protect the nozzle flow from upstream pressure effects induced by combustion in the test section. Wall pressure ports are placed in the isolator to measure the degree of upstream interaction produced by combustion in the chamber. Optical access is available to the isolator's flow from three sides. The test section is symmetric with ample optical access through side windows. The cross section is 2.5 × 2.5 cm upstream of a step that has a height H of 12 mm. A constant cross-sectional duct follows for $10H$, and continues with a diverging duct for the next $16H$.

The flameholding and fuel-injection configuration is shown in Fig. 4, including a schematic of the isolator and combustor. Note that the combustor is symmetric about the line shown in the Fig. 4 but injection only occurred from one side. Fuel was injected from the step base parallel to the flow and from the isolator at $-10H$. Fuel was also injected downstream of the step at the $4H$ location for comparison with isolator injection. The pilot injection provides a method of fueling the recirculation region for flameholding. Gaseous hydrogen has been used as the pilot flame in this study due to its broad

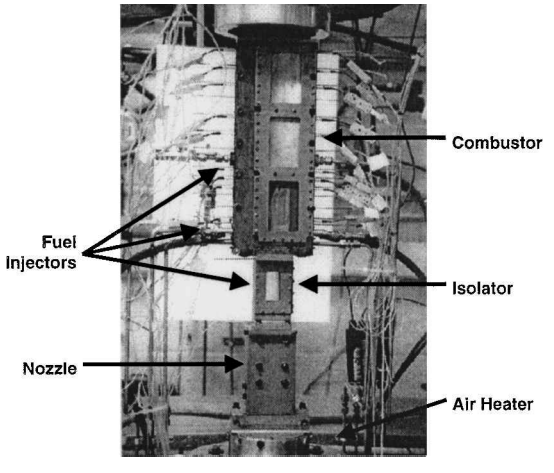

Fig. 2 Experimental facility: Mach 1.6–3.6, $P_{0,air}$ = 1–10 atm, $T_{0,air}$ = 300–1200 K; combustion chamber entrance cross section is 2.5 × 2.5 cm^2; four possible fuel injection locations, independently controlled; fuzzy logic based temperature controller.

flameholding domain in terms of equivalence ratio and flow conditions at the flameholder location, namely, velocity, temperature, and pressure.[10] The pilot-H_2 is injected from nine 0.8-mm-diam sonic orifices and was ignited with an electric spark. The injection ports in the isolator and downstream of the step were 1.5 mm. Figure 4b shows a detail of the pylon geometry. A pyramid shape has been selected with a base width equal to 1.5 times the jet diameter, and the orifice center is placed at one jet diameter downstream of the pylon face. The pylon height was chosen close to a quarter of the duct height. Because of the proximity of the pylon to the exit of the supersonic nozzle (3 cm) the thickness of the boundary layer and the cross-sectional pressure distribution at the pylon's location are not substantially different than indicated in Fig. 3. The fuel mass flow for gaseous fuels was computed by use of the measured total supply pressures and temperatures and the corrected sonic area of the orifice determined from calibration of the injector discharge coefficient. For liquid fuels, the mass flow was measured directly via a turbine flowmeter.

Results

Effects of Liquid Injection on Mixing Without Combustion

Figure 5 shows plots of the normalized total pressure distributions at the exit of the isolator with the pylon installed, acquired by traversing a pitot probe across the isolator exit and normalized by the stagnation chamber total pressure, which ranged during these tests between 4.8 and 5.1 atm. Note that the Z direction is perpendicular to the contoured faces of the nozzle and the Y direction is parallel to the contoured faces of the nozzle. The pylon protrudes into the flow along the X direction. Note from this plot and by comparison with Fig. 3 that the pylon introduces minimal pressure distortions in the flow.

Figure 6 shows shadowgraph images of the cold, noncombusting flowfield in the isolator with liquid (water) injection without the pylon (Fig. 6a) and behind the pylon (Figs. 6b and 6c). Although the liquid has been injected at the same dynamic pressure ratio, $q_{\text{jet/air}} = 0.7$, without and with the pylon in Figs. 6a and 6b, the pylon

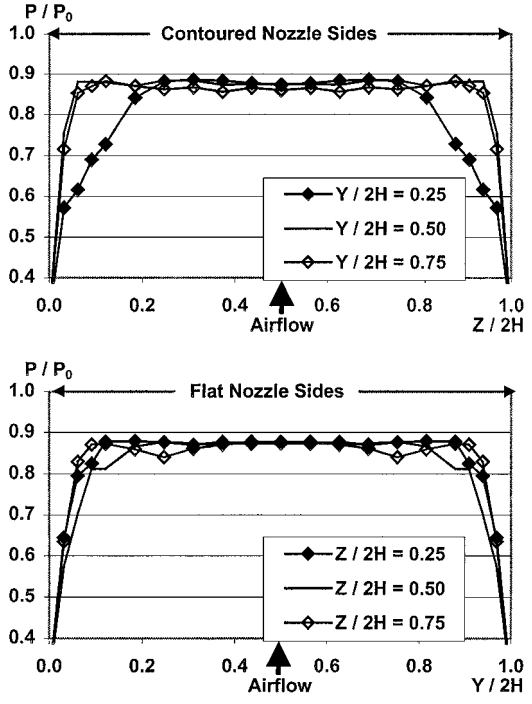

Fig. 3 Nozzle exit total pressure profiles normalized by the stagnation chamber total pressure: Z direction is perpendicular to contoured sides of nozzle and Y direction is parallel to contoured sides of nozzle.

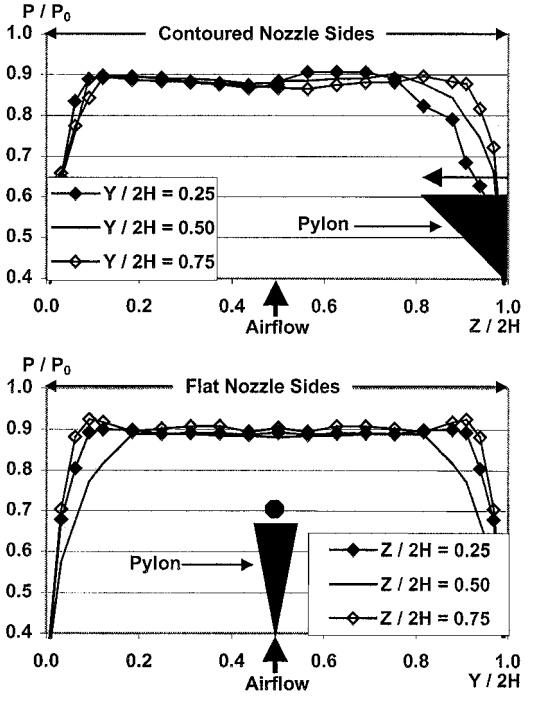

Fig. 5 Isolator exit total pressure profiles normalized by stagnation chamber total pressure; location and orientation of pylon are indicated: Z direction is perpendicular to contoured sides of nozzle and the Y direction is parallel to contoured sides of nozzle.

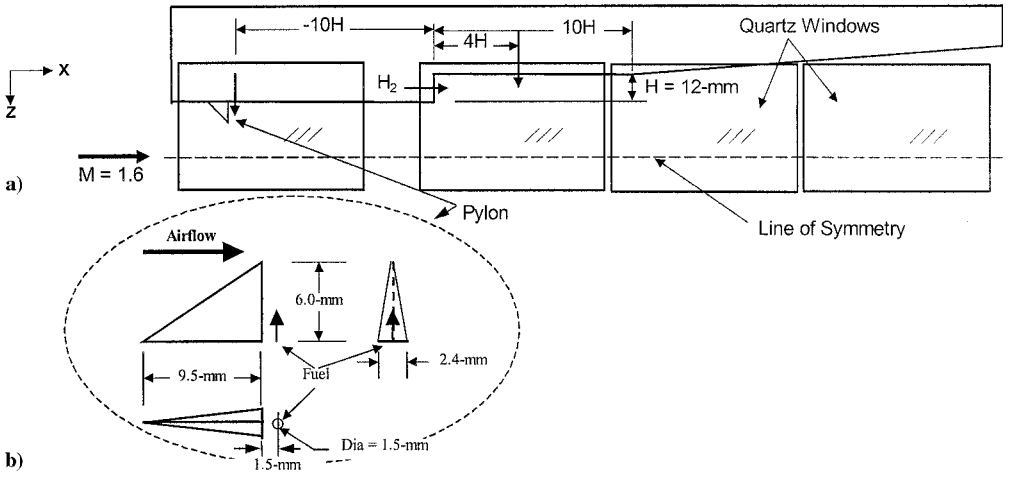

Fig. 4 Injection and flameholding configurations; combustor is geometrically symmetric with fuel injected from one side only: a) isolator and combustor schematic and b) pylon geometry.

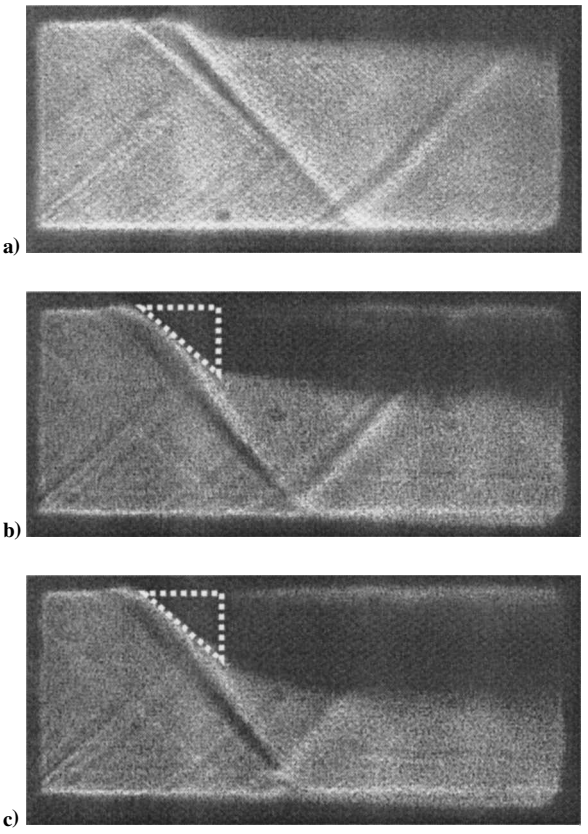

Fig. 6 Noncombusting liquid (water) Injection in the isolator: a) without pylon $q_{jet/air} = 0.7$, b) behind pylon $q_{jet/air} = 0.7$, and c) behind pylon $q_{jet/air} = 1.3$; dashed white lines indicate pylon location.

has clearly contributed to increase the penetration with the liquid immediately penetrating to the pylon's height. In previous studies of transverse injection in supersonic flows,[11] it was indicated that the penetration height-to-jet diameter ratio h/D_{inj}, of a liquid in air, at similar Mach numbers, scales with the square root of the dynamic pressure ratio of the jet to the freestream $q_{jet/air}$ defined as

$$q_{jet/air} = \frac{(\dot{m}^2/A^2\rho)_{jet}}{(\gamma p M^2)_{air}} \tag{1}$$

For injection without the pylon, the liquid penetrated to a $h/D_{inj} = 1.8$ at 2.5 jet diameters downstream of the jet. However, the presence of the pylon contributes significantly to increase the liquid penetration, with the jet penetrating immediately on injection to beyond the pylon height, $h/d_{inj} = 5.6$ at 2.5 jet diameters. Most important, note in Fig. 6b that the presence of the pylon helped remove all of the liquid from the wall surface, in contrast to the case without the pylon in Fig. 6a, which is significant for the elimination of potential flashback. Further increasing $q_{jet/air}$ to modest values of 1.3 (Fig. 6c) showed a significant increase in penetration with minimal effects on the isolator shock train.

Figure 7 shows shadowgraph images of the noncombusting flowfield in the combustion chamber. The step is visible in the left upper side off the images. Liquid has been injected into the isolator directly from the wall, (Fig. 7a) and behind the pylon (Fig. 7b) at the same dynamic pressure ratio, $q_{jet/air} = 0.5$. In Fig. 7b there is only a slightly shaded area in the core of the air entering the combustion chamber, indicating that a significant degree of mixing has occurred, thus the absence of strong gradients that would become visible in the shadowgraph. Quite in contrast, Fig. 7a indicates that, without the pylon, the liquid has remained largely in the region near the injection wall, appearing in the image as the rich dark region of the shear layer formed at the boundary between the recirculation region and the high-speed core flow.

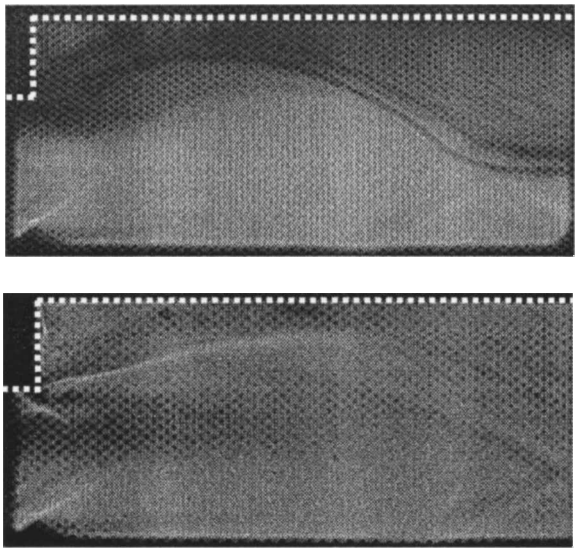

Fig. 7 Combustor views with noncombusting liquid (water) injection in the isolator, $q_{jet/air} = 0.5$: a) without pylon and b) behind pylon; dashed white lines indicate step and combustor wall.

Effects of Pylon Assisted Injection on Combustion and Heat Release

Liquid JP-10

Combustion tests with JP-10 injection from the isolator took place at three air stagnation temperatures: 300, 600, and 900 K. Hydrogen has been used as a pilot flame with low equivalence ratios adjusted to remain close to the stoichiometric conditions in the recirculation region as evidenced by the temperature measurement at $\frac{1}{2}H$ downstream of the step in the recirculation region.[12] The pilot-H_2 equivalence ratio has been adjusted to an overall $\Phi_{H2} = 0.02$, resulting in a local temperature at the beginning of JP-10 injection of 1700 K. As the air temperature increased, the mixture became richer in the recirculation region and flameholding became restricted to lower ranges of liquid injection. Figure 8 shows shadowgraph images taken in the isolator for JP-10 injection and combustion in air at 300 K. Figures 8a and 8b have been taken for JP-10 equivalence ratios of 0.26 ($q_{jet/air} = 0.08$) and 0.41 ($q_{jet/air} = 0.19$), respectively. Note that at these moderate fuel flow rates the effect of fuel injection on the isolator shock train was minimal, with no visible change in the shock strengths. The combustion in the test section remains well isolated with no upstream effects noticeable. As the fuel equivalence ratio was increased to 0.53 ($q_{jet/air} = 0.31$), the mass addition in the isolator resulted in flow choking, as evidenced in Fig. 8c.

The combustion chamber wall pressure distributions at 300 and 600 K are shown in Fig. 9, normalized by the static pressure at the nozzle exit. The static pressure at the nozzle exit was measured in all experiments at $x/h = -13$. In the data shown in Fig. 9, this pressure ranged between 2.33 and 2.57 atm. At 600 K, the pilot-H_2 equivalence ratio has been maintained at 0.02 by reducing the H_2 flowrate. The temperature in the recirculation region behind the step was 1900 K in this case. Because of increased vaporization of the liquid JP-10 when injected into the higher temperature air, the volumetric expansion of the jet plume increased, resulting in the lower combustor entrance Mach number evidenced by the increased pressure at the isolator exit for the $T_{0,air} = 600$ K case. The pressure rise in the combustor decreased with increasing air stagnation temperature due to enrichment of the combustion region. This resulted in a lower local pressure, as evidenced by the pressure measurement in the base, resulting in an increased flow turning angle at the step.

At 900 K, the flame was very susceptible to flameout even for small amounts of JP-10 flowrate. Combustion of JP-10 at 900 K was obtained by following the procedure indicated by the time trace shown in Fig. 10. The temperatures and the equivalence ratios indicated in Fig. 10 have been recorded with accuracy of ± 1.3 K and from ± 2.8 to 3.6%, respectively, with higher equivalence ratio accuracy for liquid JP-10 and less for gaseous ethylene. Initially, the air

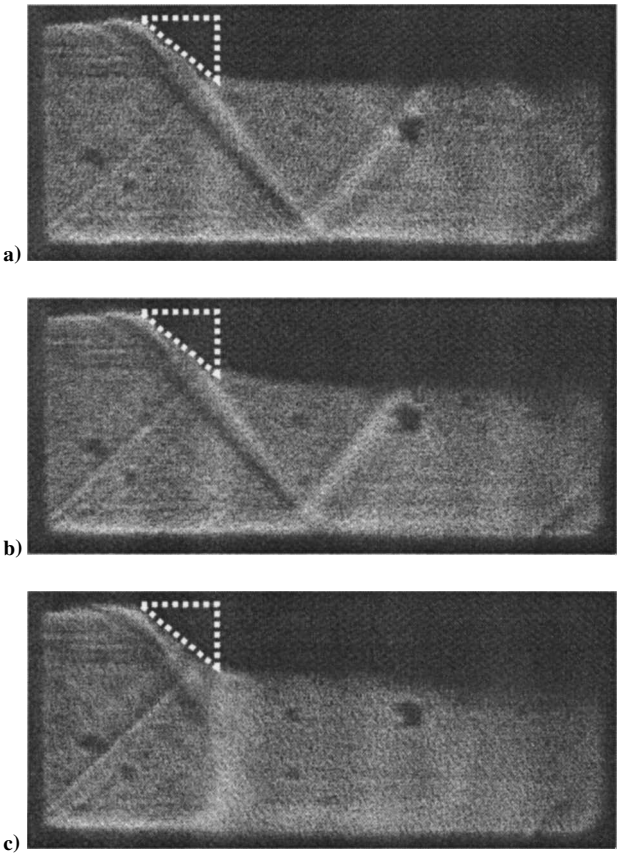

Fig. 8 Isolator views with JP-10 injection and combustion ($T_{0,air}$ = 300 K, Φ_{H2} = 0.02): a) $\Phi_{JP\text{-}10}$ = 0.26, b) $\Phi_{JP\text{-}10}$ = 0.41, and c) $\Phi_{JP\text{-}10}$ = 0.53; dashed white lines indicate pylon location.

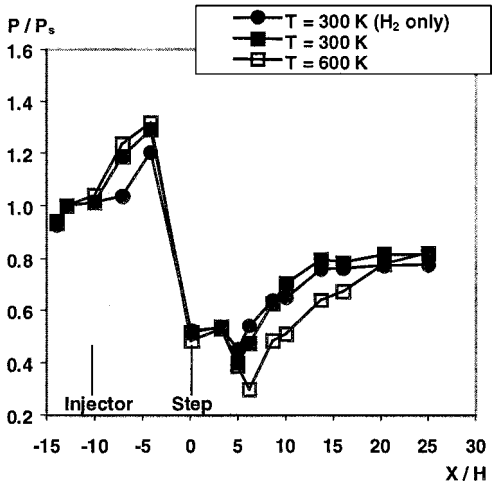

Fig. 9 Combustor normalized pressure distribution for JP-10 injection in isolator at two different air stagnation temperatures; H_2 only combustion is shown for comparison (Φ_{H2} = 0.02, $\Phi_{JP\text{-}10}$ = 0.2).

stagnation temperature was set at 600 K and the JP-10 equivalence ratio to a moderate value, $\Phi_{JP\text{-}10} = 0.05$. The air stagnation temperature was then slowly ramped up with the JP-10 flowrate adjusted to $\Phi_{JP\text{-}10} = 0.2$. This value was maintained constant as the temperature was increased in the 700–900 K interval. The JP-10 flowrate was increased to bring the overall equivalence ratio to 0.35, resulting in rich flameout.

Along with improved penetration and mixing, the question of combustion efficiency of this injection scheme arises. Although the combustion efficiency was not calculated here, the wall pressure distribution is used to indicate the amount of heat release from combustion. Figure 11 shows the normalized combustor pressure

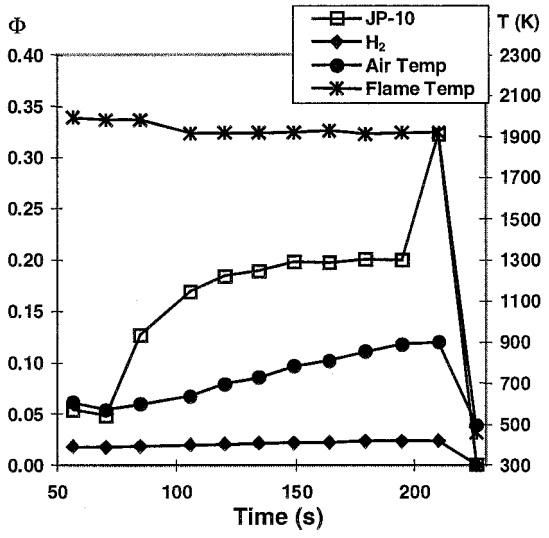

Fig. 10 Time trace of experimental parameters during JP-10 injection and combustion for $T_{0,air}$ = 600–900 K. Initially, $T_{0,air}$ = 600 K and $\Phi_{JP\text{-}10}$ = 0.05. $T_{0,air}$ was then slowly ramped up with JP-10 flowrate adjusted to $\Phi_{JP\text{-}10}$ = 0.20; this value was maintained constant as $T_{0,air}$ was increased in 700–900 K interval; JP-10 flowrate was increased to bring overall $\Phi_{JP\text{-}10}$ to 0.35 resulting in rich flameout.

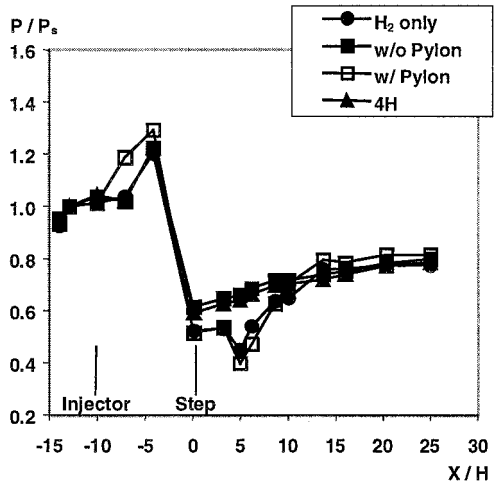

Fig. 11 Combustor normalized pressure distribution for JP-10 injection in isolator with and without pylon and at 4H location, $T_{0,air}$ = 300 K, H_2 only combustion is shown for comparison (Φ_{H2} = 0.02, $\Phi_{JP\text{-}10}$ = 0.2).

distribution for JP-10 injection 1) in the isolator behind the pylon, 2) in the isolator without the pylon, and 3) directly into the combustion chamber transverse to the flow at the 4H location. The static pressure at the nozzle exit for these tests ranged from 2.47 to 2.57 atm. In all three cases, the air stagnation temperature has been maintained at 300 K to emphasize the effects of heat release on the Mach number reduction. The JP-10 equivalence ratio has been maintained at 0.2 in all cases. Note that injection in the isolator without the pylon and injection at the 4H location show similar pressure profiles immediately downstream of the step in the recirculation region, which indicates the capture of significant amounts of JP-10 into the recirculation region, contributing to the increased heat release in this region. Injection behind the pylon and the H_2 only case show similar pressure profiles immediately downstream of the step in the recirculation region, indicating the presence of only minimal amounts of JP-10 in the recirculation region with only minimal contribution to the heat release. This indicates the effectiveness of injection behind the pylon in placing most of the injected fuel within the core flow. The highest pressure rise in the far field, that is, at the 15H location and beyond, occurs for injection behind the pylon in the isolator.

Gaseous Ethylene

Ethylene has been injected from the isolator both without the pylon and behind the pylon. Figure 12 shows shadowgraph images of ethylene injection in the isolator without the pylon in Fig. 12a and behind the pylon in Fig. 12b. Both images were taken at $\Phi_{C2H4} = 0.2$, $q_{jet/air} = 3$, and $T_{0,air} = 300$ K. As indicated in the Fig. 12, injection without the pylon causes the boundary layer to separate with an evident effect on the strengthening of the shock system. Although penetration is about double for the injection behind the pylon case, the effect on the isolator shock train is less pronounced, similar to the liquid injection case. Figure 13 shows the normalized axial pressure distribution for piloted-H_2, ethylene combustion with injection in the isolator, both without and behind the pylon. The static pressure at the nozzle exit ranged for these tests between 2.54 and 2.6 atm. Hydrogen only combustion is also shown for reference. Both cases of isolator injection indicate increased pressure in the isolator due to mass addition at $-10H$ in comparison with the liquid injection (see Fig. 11) because the gaseous ethylene plume expanded much more rapidly than the liquid JP-10 plume. Without the pylon, the pressure rise in the recirculation region is reduced, indicating local enrichment and reduced combustion efficiency. Higher far-field pressures for injection behind the pylon indicate increased rates of heat release.

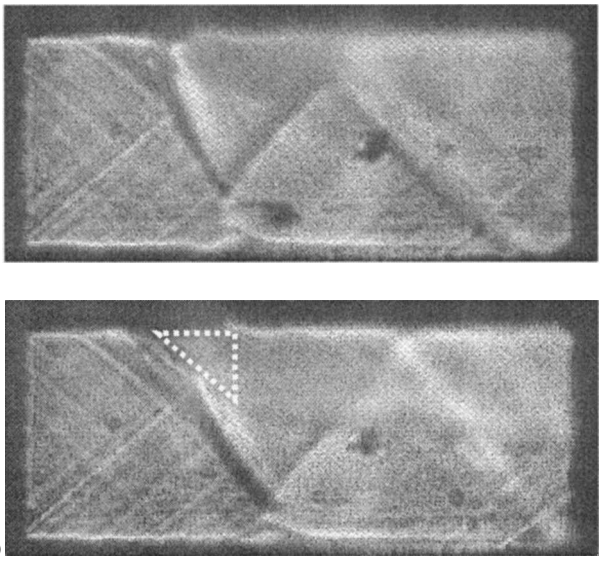

Fig. 12 Ethylene injection in isolator, $\Phi_{C2H4} = 0.2$, $q_{jet/air} = 3$: a) without pylon, b) behind pylon; dashed white lines indicate pylon location.

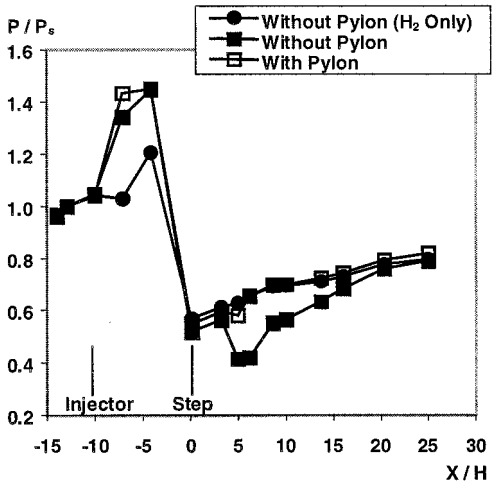

Fig. 13 Normalized combustor axial pressure distribution for ethylene injection in isolator both without and behind pylon with H_2 only combustion shown for comparison, $\Phi_{H2} = 0.02$ and $\Phi_{C2H4} = 0.2$.

Summary

Liquid JP-10 and gaseous ethylene have been injected upstream of the combustion chamber in a Mach 1.6 airflow behind a thin pylon to determine the ability of the pylon to improve penetration and mixing. This study indicated the following results:

1) The presence of thin pylons with sharp leading edges does not introduce significant pressure losses or distortion in the isolator airflow.

2) Even at moderate dynamic pressure ratios, the presence of the pylon promotes substantially higher penetration in comparison with simple wall injection.

3) Because of this increased penetration, the entire liquid jet is lifted from the wall, eliminating the danger of flashback through seeding of the boundary layers with a combustible mixture.

4) As a result of the increased penetration with injection behind the pylon, most of the liquid injected upstream of the combustion chamber penetrates into the core of the airflow, resulting in improved mixing, offering the possibility of reduced combustion chamber lengths.

5) Airflow choking with substantial effects on the isolator shock train is not observed for injected equivalence ratios under 0.5.

6) The normalized wall pressure distribution indicates higher rates of heat release in the far field for the cases involving injection behind the pylon, an indication of improved combustion efficiency through improved mixing.

7) Ethylene injection and combustion indicates a substantial increase in penetration over the basic wall injection case with reduced effects on the isolator shock train.

References

[1]"Design Analysis of the Model Hydrocarbon Fueled Engine Performance," John Hopkins Univ. Applied Physics Lab., Final Contractor Rept. 700-773723, conducted by New Technologies Implementation Center—Central Inst. of Aviation Motors, June 1999.

[2]Northam, G. B., and Anderson, G. Y., "Supersonic Combustion Ramjet Research at Langley," AIAA Paper 86-0159, 1986.

[3]Baranovski, S. I., and Schetz, J. A., "Effect of Injection Angle on Liquid Injection into Supersonic Flow," AIAA Paper 79-0383, 1979.

[4]Northam, G. B., Capriotti, D. P., Byington, G. B., and Greenberg, I., "Evaluation of Parallel Injector Configurations for Mach 2 Combustion," *Journal of Propulsion and Power*, Vol. 8, No. 2, 1992, pp. 491–499.

[5]Marble, F. E., Zukoski, E., Jacobs, J. W., Hendrics, G. J., and Waitz, I. A., "Shock Enhancement and Control of Hypersonic Mixing and Combustion," AIAA Paper 90-1981, 1990.

[6]Vinogradov, V. A., and Prudnikov, G. A., "Injection of Liquid into the Strut Shadow at Supersonic Velocities," Society of Automotive Engineers, Paper SAE-931455, April 1993.

[7]Livingston, T., Segal, C., Schindler, M., Owens, M. G., and Vinogradov, V. A., "Penetration and Spreading of Liquid Jets in an External–Internal Compression Inlet," *AIAA Journal*, Vol. 38, No. 6, 2000, pp. 989–994.

[8]Owens, M. G., Tehranian, S., Segal, C., and Vinogradov, V. A., "Flameholding Configurations for Kerosene Combustion in a Mach 1.8 Airflow," *Journal of Propulsion and Power*, Vol. 14, No. 4, 1998, pp. 456–461.

[9]Segal, C., and Young, C. D., "Development of an Experimentally-Flexible Facility for Mixing–Combustion Interactions in Supersonic Flow," *Journal of Energy Resources Technology*, Vol. 118, No. 1, 1996, pp. 152–158.

[10]Ozawa, R. I., "Survey of Basic Data on Flame Stabilization and Propagation for High Speed Combustion Systems," Air Force Aeropropulsion Lab., TR-70-81, Wright–Patterson Air Force Base, Ohio, Marquart Co., Jan. 1971.

[11]Arai, T., and Schetz, J. A., "Injection of Bubbling Liquid Jets from Multiple Injectors into a Supersonic Stream," *Journal of Propulsion and Power*, Vol. 10, No. 3, 1994, pp. 382–386.

[12]Ortwerth, P. J., Mathur, A. P., Segal, C., Mullagiri, S., and Owens, M.G., "Combustion Stability Limits of Hydrogen in a Non-Premixed, Supersonic Flow," International Symposium on Air Breathing Engines, Paper ISABE 99-143, 1999.